Rare Metal Materials and Engineering
Volume 55, Issue 6, June 2026
Available online at www.rmme.ac.cn

Science Press

Cite this article as: Ma Xiaolu, Wang Siyu, Shen Boran, et al. Design, Properties, and Multi-field Application Progress of Porous Structures of NiTi Shape-Memory Alloy Prepared by Selective Laser Melting[J]. Rare Metal Materials and Engineering, 2026, 55(06): 1451-1464. DOI: https://doi.org/10.12442/j.issn.1002-185X.20250309.

REVIEW

Design, Properties, and Multi-field Application Progress of Porous Structures of NiTi Shape-Memory Alloy Prepared by Selective Laser Melting

Ma Xiaolu[1,2], Wang Siyu[1], Shen Boran[1], Wu Wenzheng[1], Li Guiwei[1]

[1] School of Mechanical and Aerospace Engineering, Jilin University, Changchun 130025, China; [2] College of Mechanical and Vehicular Engineering, Changchun University, Changchun 130022, China

Abstract: NiTi shape-memory alloys are extensively used across various fields due to their distinctive shape-memory effect and superelasticity. Additive manufacturing technique enables the precise fabrication of high-performance complex structures of NiTi shape-memory alloys, facilitating innovative structural designs. This paper reviewed the applications of NiTi porous structures prepared by selective laser melting (SLM) in the fields of biomedical and mechanical engineering. It summarized the characteristics of various novel porous structures of SLM-NiTi across various applications, explored innovative design methodologies for these structures, and discussed their corresponding advantageous properties, which include compressive performance, superelasticity, shape-memory effect, energy absorption capability, and biocompatibility. These design methodologies and structures can provide references for the design and application of high-performance NiTi structures prepared by additive manufacturing.

Key words: NiTi shape-memory alloys; selective laser melting; porous structures

1 Introduction

Nickel-titanium (NiTi) has rapidly emerged as an attractive functional material, which is widely used due to its unique advantages, including the distinctive shape-memory effect, superelasticity, damping properties, and biocompatibility[1–2]. However, the high ductility, strength, rebound effect, and work hardening[3] characteristics of NiTi pose challenges in achieving optimal 3D structural effects, thereby restricting its application across various fields[4–5]. The advent and continuous advancement of additive manufacturing technique have enhanced the processability of NiTi, facilitating the realization of higher precision in the fabrication of complex 3D structures[6].

In addition, additive manufacturing technique has significantly advanced the design and performance investigation of high-performance porous structures, including NiTi alloy lattices and honeycombs, across diverse disciplines. These structures exhibit remarkable advantages in biomedical bone implants and engineering energy-absorbing components, highlighting their interdisciplinary application potential[7–9]. This synergy between material properties and structural advantages manifests in several key attributes: high deformation and recovery capabilities, biocompatibility, load-bearing capacity, and energy absorption performance, providing a new two-dimensional approach for high-performance structural design. Most research teams tend to review the material properties, microstructures, and manufacturing process parameters of NiTi[3–4,10–13]. Whereas literature reviews focusing on application scenarios remain disproportionately scarce, with explorations into the design methodologies and performance advantages of NiTi alloy porous structures being particularly restricted.

Thus, this review taken NiTi-based multifunctional structures and their design methodologies as the entry point. Based on different application contexts, it critically reviewed the characteristics of novel structures, such as lattice and honeycomb structures fabricated by SLM for NiTi alloys in

Received date: June 03, 2025
Foundation item: Supported by Jilin Provincial Department of Education (JJKH20240737KJ)
Corresponding author: Wu Wenzheng, Ph. D., Professor, School of Mechanical and Aerospace Engineering, Jilin University, Changchun 130025, P. R. China, E-mail: wzwu@jlu.edu.cn

biomedical and mechanical engineering fields, as shown in Fig. 1. The review also explored the innovative structural design methods and the resultant superior properties, including mechanical properties, superelasticity, shape-memory effect, energy absorption capacity, and biocompatibility. Finally, this review put forward critical analysis and future prospects.

2 Biomedical Field: Structures of Human Bone Implant

For human bone implants, the mechanical properties and biocompatibility are critical factors that determine the therapeutic effect of implants[14]. The elastic modulus is a fundamental mechanical property that significantly affects overall performance. When the elastic modulus of an implant exceeds that of human bone, it can lead to adverse effects, such as stress shielding and bone resorption, ultimately resulting in treatment failure[15–16]. Notably, 316L stainless steel exhibits favorable mechanical properties and machinability, while Ti6Al4V demonstrates excellent biocompatibility as a titanium alloy. Both materials are widely used in the fabrication of bone implants[17]. However, the elastic modulus and stiffness of these implants differ considerably from those of human bone, which can induce stress shielding at the implant site and potentially cause secondary injuries. Furthermore, harmful substances, such as aluminum and vanadium, may be released into the body, leading to additional harm[18–20]. The relevant performance parameters of human bone are summarized in Table 1[7,21–22].

The biocompatibility of the implant is crucial for the effective attachment of bone cells in the affected area and their subsequent high activity, which promotes the bone healing process[23]. In the case of 316L stainless steel, its low biocompatibility hinders normal bone cell growth on the surface of the structure, thereby delaying the healing process[24]. Moreover, the structural characteristics, such as the small specific surface area, further restrict the attachment area for cells, consequently reducing the treatment rate[25].

Currently, the challenges associated with the elastic modulus and biocompatibility of bone implants can be addressed through both material selection and the design of porous structures. Research indicates that the porosity and pore size of the structure are critical determinants of the biocompatibility of bone implants, directly influencing cell movement and tissue growth. An optimal combination of porosity and pore size can enhance the specific surface area of the structure, increasing the number of attached osteocytes and facilitating the healing process. Furthermore, higher porosity can lower the elastic modulus of the structure, allowing for the establishment of a quantitative relationship between porosity and elastic modulus, such as the Gibson-Ashby model[26], and enabling the elastic modulus of the

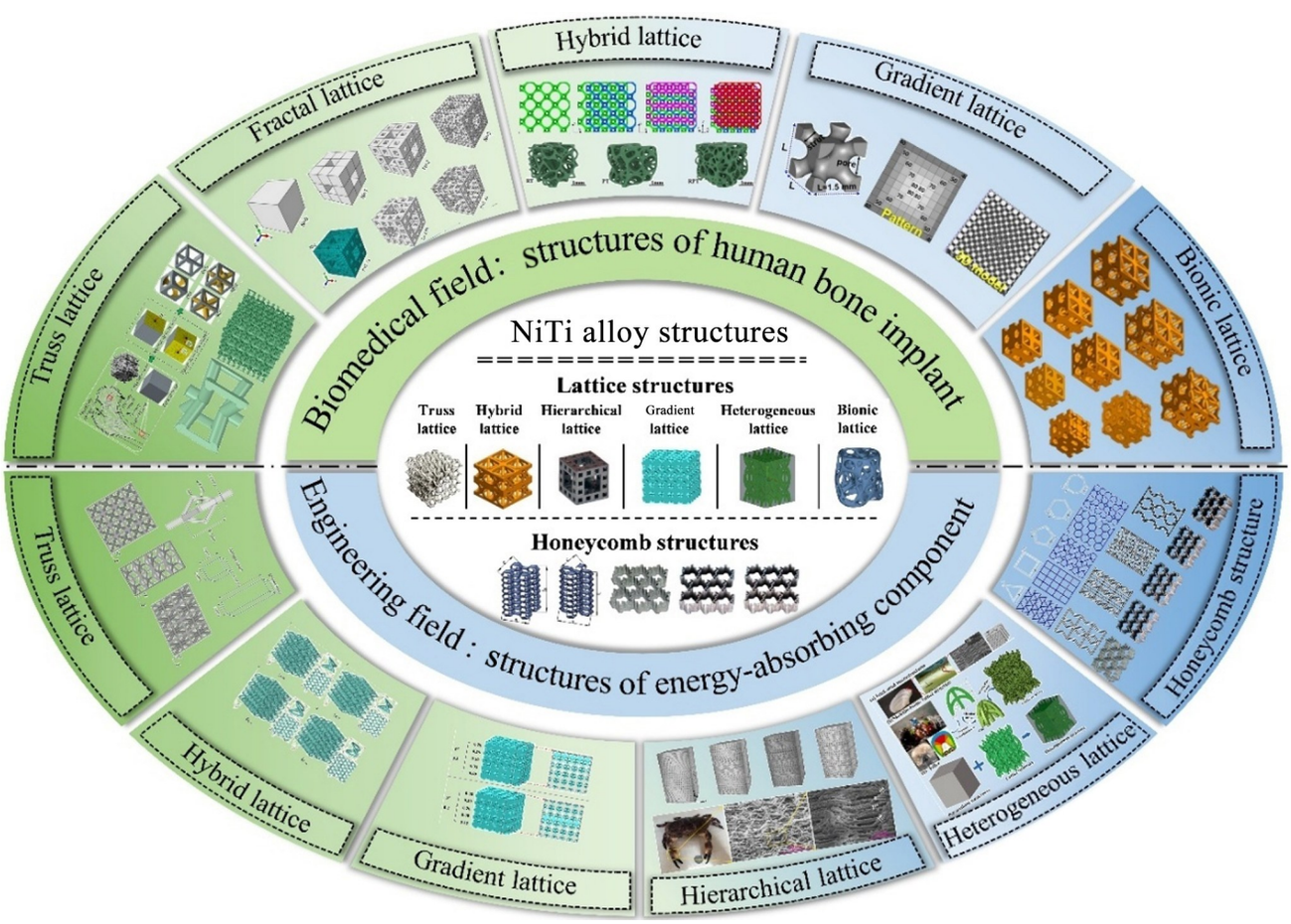

Fig.1 Schematic illustration of structure characteristics, design principles, and applications of various NiTi alloy structures

Table 1 Comparison of mechanical properties of human bone[21]

Bone	Porosity	Elastic modulus/GPa		Strength/MPa		Poisson's ratio	Range of pore diameter
Cortical bone	3%–5%	Vertical	17.9±3.9	Tensile	135±15.6	0.40±0.16	260–510 μm: fibrosis of new bone is promoted[22].
				Compressive	205±17.3		
		Horizontal	10.1±2.4	Tensile	53±10.7	0.62±0.26	
				Compressive	131±20.7		
Cancellous bone	Approximately 90%	Shear	3.3±0.4	Shear	65.0±4.0	-	300–900 μm: bone ingrowth and blood vessel formation are promoted[7].
		Centrum	0.067±0.045		2.4±1.6		
		Tibia	0.445±0.257		5.3±2.9		
		Femur	0.441±0.271		6.8±4.8		

structure to be adjusted within a specific range.

The determination and characterization of structural mechanical properties and biocompatibility are analogous to existing studies. In terms of mechanical properties, the characterization of compression behavior is mainly conducted through by quasi-static uniaxial compression experiments, which elucidate the stress-strain curve of the structure. The superelasticity and shape-memory properties of the porous structure, in conjunction with NiTi, both emphasize the deformation recovery of the post-unloading structure. However, the characterization process for superelasticity is centered on cyclic stress factors, while that for the shape-memory effect focuses on temperature factors[27]. Biocompatibility largely depends on the permeability of the structure and the characteristics of cellular activity. Fig. 2 illustrates the principles and test results related to mechanical properties and biocompatibility[26,28–31]. The symbol meanings are described in related references.

In recent years, many research teams have enhanced the mechanical properties, deformation recovery, and biocompatibility of structures through innovative design methodologies. This section reviews novel structural design methods for bone implants, analyzes the performance advantages of each structure, and elucidates their application potential in comparison to existing structures within the domain of human bone implants. The structural features and key performances of each structure are shown in Table 2[5,29,31–34].

2.1 Truss lattice

The truss lattice is typically composed of elements such as rods and nodes, with each rod interconnected by nodes. Due to its simple structural features, truss structure is widely used in the field of biomedical scaffolds, which facilitates geometric design and mechanical analysis and establishes the connection between these two parts. Typical examples of this structural type include body-centered cubic (bcc) and face-centered cubic (fcc) structures. Although these structures have simple structural characteristics that facilitate design and enable the exploration of the relationship between structural parameters and performance[35], they also result in cross-sectional discontinuities at the nodes, which can lead to stress

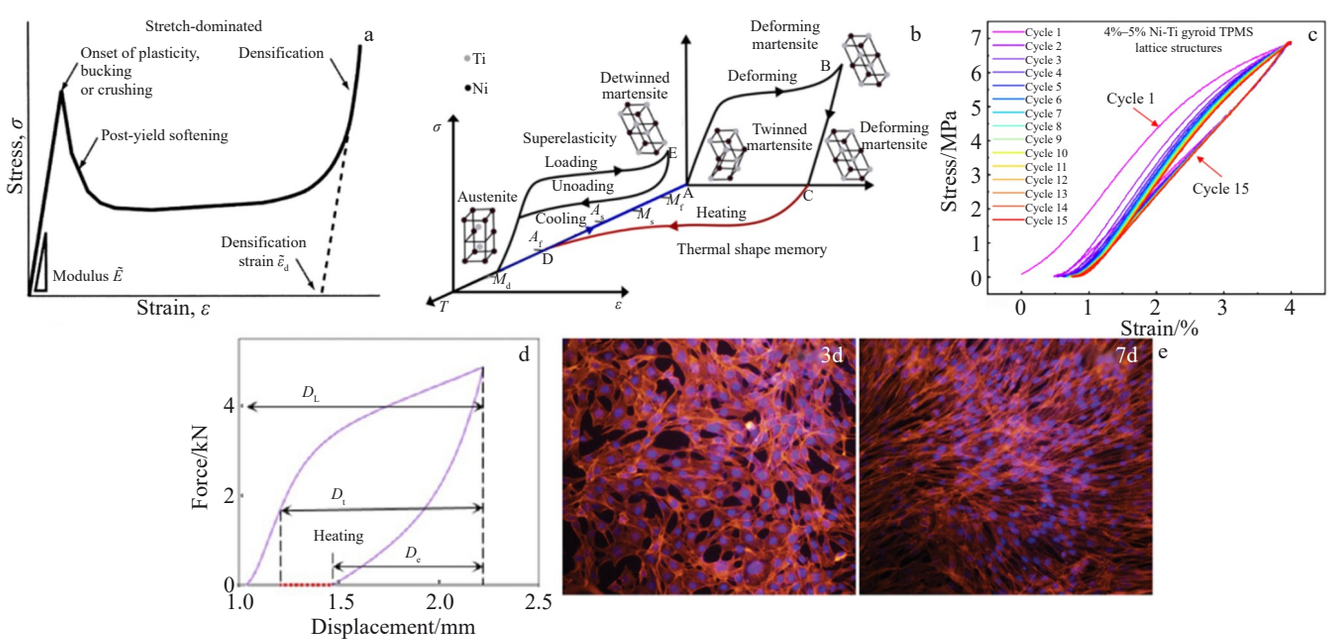

Fig.2 Principles and characterization results of mechanical properties and biocompatibility: (a) stress-strain curve of the structure[26]; (b) austenite-martensite phase transformation process and lattice structure changes[28]; (c) NiTi hyperelastic properties[29]; (d) NiTi shape-memory effect[30]; (e) biocompatibility results of NiTi bone implants[31]

Table 2 Structure features and key performances of lattice structures of human bone implants

Structure feature	Key performance	Ref.	Structure feature	Key performance	Ref.
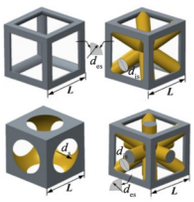	The quantitative mathematical relationship between the structural parameters (d_s, d_{is}, and d_{es}) and the degree of anisotropy of the elastic modulus is constructed.	[32]	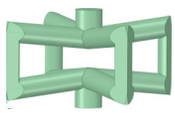	A negative Poisson's ratio of −0.003 23 is obtained. The recovery rate of superelasticity is about 75.7%.	[33]
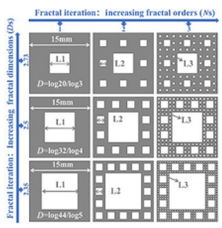	The structure shows a superelasticity deformation recovery rate of 93.93% – 98.27% under the conditions of 2.35≤D≤2.5 and 2≤N≤3.	[5]	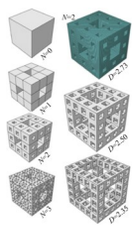	The compressive modulus can vary between 0.96–25.3 GPa. The recoverable strain is increased by 2 – 6 times compared with that of natural bones.	[34]
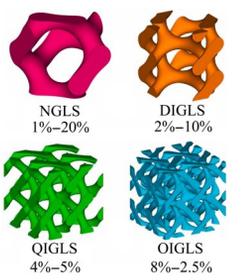	The compressive modulus can vary between 152.55–835.15 MPa. The structure shows a superelastic deformation recovery rate of 98.87% – 99.46%.	[29]		When the structural porosity is 83.1%, the compressive modulus is 798.1 MPa, which is within the range of the elastic modulus of human bone. After the structure is implanted into the hip joint, it exhibits nearly 100% cell activity. The structural features are consistent with those of human bones.	[31]

Note: the symbols and abbreviations in Table 2 are explained in the corresponding references.

concentration during loading, consequently diminishing structural strength[36–37]. Furthermore, their properties, such as anisotropy, deformability, and strength, differ significantly from those of human bone, making traditional truss lattices challenging to apply in human bone implants. Consequently, various researches in innovative design and structural function studies related to truss lattices have been conducted.

Farber et al[33] demonstrated that the truss lattice exhibits a negative Poisson's ratio of −0.003 23, thereby mitigating the secondary damage to human tissues associated with the expansion characteristics of positive Poisson's ratio[38–39], and indicating superior superelasticity compared to traditional truss structures. Kang et al[32] established a mathematical mapping relationship between structural parameters and anisotropy, reducing the discrepancy in elastic modulus anisotropy between truss lattices and human bone. Table 3 illustrates the fitting formula and its goodness of fit[32].

The truss lattice has been optimized in various ways, leading to enhanced performance. However, due to its inherent structural characteristics, the truss lattice exhibits low performance across multiple aspects, including increased stress concentration and reduced deformation capacity. It remains challenging to match the characteristics and performance of human bone.

Table 3 Fitting formula and goodness of fit of structural parameters and elastic modulus[32]

Structure	Function
	$f_{DA-CSH}=f(d_s)=4.065d_s^2-22.07d_s+30.47$, R^2=0.997
	$f_{DA-OGC}=f(d_{es})=1.268d_{es}^2-0.608d_{es}+0.2$, R^2=0.999
	$f_{DA-bcc}=f(d_{is},d_{es})=2.633d_{es}^2-5.46d_{is}^2+4.434d_{is}d_{es}-8.573d_{es}+4.558d_{is}+4.932$, R^2=0.999
	$f_{DA-rbcc}=f(d_{is},d_{es})=3.272d_{es}^2-3.672d_{is}^2+3.931d_{is}d_{es}-8.252d_{es}+2.5888d_{is}$, R^2=0.987

Note: the symbols and abbreviations in Table 3 are explained in Ref.[32].

2.2 Fractal lattice

Compared with the truss structure, fractal lattices are equivalent to designing a periodic hole structure on the truss

member elements, which is inspired by natural porous structures such as bones, and characterized by a significant parametric design process[35]. Their performance can be modulated through parameters, such as fractal dimension and fractal order[5,34]. The Menger sponge is the most prominent fractal lattice structure in recent years, with various research teams investigating the relationship between its structural properties and parameters like fractal dimension (*D*) and fractal order (*N*).

Zhao[5] and Zhang[34] et al both investigated the Menger sponge fractal structure, demonstrating superior tunability for cancellous bone compared to traditional truss structures. In contrast, Zhang et al[34] explored the performance variation range of the Menger sponge. Zhao et al[5] investigated the variation trend of superelasticity in Menger sponge fractal structures with respect to fractal dimension and iteration times. The fractal lattice structure shows potential in enhancing the compatibility of bone implants with natural bone. Both fractal dimension and iteration times can be systematically controlled via finite element analysis or structural design algorithms, enabling a parametric design methodology.

2.3 Hybrid lattice

Biomedical scaffolds with simple structures similar to the above two structures often have specific application scenarios to leverage their advantages, but such structures often fail to meet the multi-faceted performance requirements of biomedical scaffolds and have relatively low design freedom. The hybrid lattice structure has been found to compensate for the abovementioned defects. The hybrid lattice is defined as a structure formed by the specific mixing of elementary structures across a certain scale. This includes linear fusion in one-dimensional space and uniform fusion in three-dimensional space. This type of structure can be composed of two or more elementary structures, which may be of the same type or different types. The hybrid lattice can synthesize the performance of the elementary structures and further optimize additional aspects based on this integration[35].

Triply periodic minimal surface (TPMS) structure is one of the most common elementary structures for fusion structure design. It features a complete parametric modeling approach and primarily focuses on the fusion of two or more structures to achieve comprehensive performance enhancement[40–41]. The fusion method of a single TPMS elementary structure was examined, as shown in Fig. 3, proposing a novel design approach for TPMS hybrid lattice inspired by traditional Chinese Taoist philosophy[29]. Interlacing traditional gyroid-TPMS structures to form an integral staggered structure addresses the issue of significant residual strain during the superelastic deformation of TPMS. This configuration enhances the fatigue life of bone implants under small deformations. Compared with a single TPMS structure, the fusion design of multiple elementary structures amplifies the advantages of basic structures.

Fig. 4 shows a lattice structure designed by reverse engineering, which aligns the characteristics of bone implants with those of human bones[31,42]. The structure of trabecular bone is extracted using micro-computed tomography technique, leading to the development of a rod-plate hybrid lattice with controllable performance, based on its rod-like and plate-like trabecular structures. The structure achieves higher strength levels at lower elastic modulus. In vivo implantation in the hip joint demonstrates nearly 100% cell viability, indicating excellent biocompatibility[31]. Ref. [42] identified that the combinations of 85% porosity with a trabecular bone diameter of 900 μm and 80% porosity with a diameter of 500 μm represent the optimal structural parameters, showcasing greater application potential in bone implant structures.

2.4 Gradient lattice

For bone implants, the gradient design of the implant structure is particularly important. If the implant fails to well meet the pore structure characteristics of the gradient changes in the surrounding bone tissue, it will lead to stress

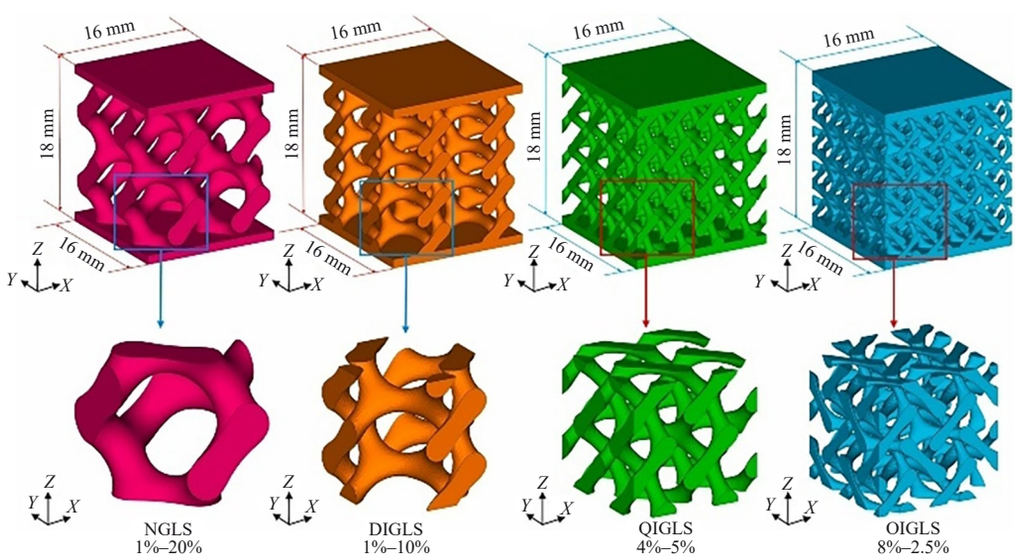

Fig.3 Novel hybrid lattices of TPMS based on traditional Chinese Taoist philosophy[29]

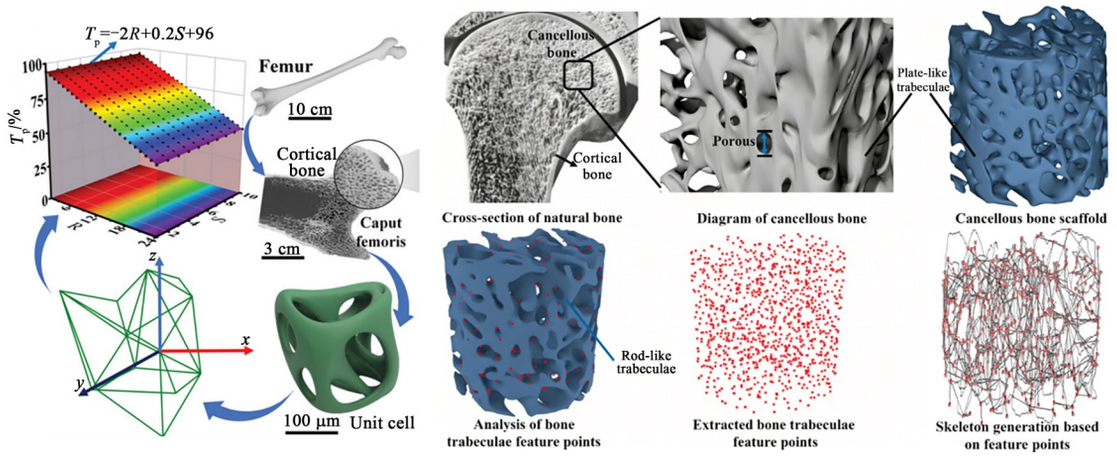

Fig.4 Reverse structural design method based on trabecular bone structure[31,42]

concentration, low cell survival rate, or implant detachment. For bone implants to achieve good therapeutic effects, they need to have a pore structure with gradient changes similar to that of natural human bones, thereby better meeting the various performance requirements of the implants and reducing the possibility of treatment failure.

The gradient lattice resembles the hybrid lattice composed of a single basic structure; however, it is composed of multiple cells with varying structural parameters, including porosity, pore size, and rod diameter. This design relies on these structural parameters to control the performance characteristics of different regions[35]. For bone implants, the gradient design of the implant structure is particularly crucial and has attracted significant attention in recent years. Because bone implants must simultaneously fulfill multiple requirements, including biocompatibility and mechanical properties, to better mimic the performance of natural human bones and to reduce the likelihood of treatment failure.

Tan et al[43] designed a functionally gradient lattice structures with porosity varying from 40% to 80% along the radial direction, exhibiting superior mechanical properties compared to non-gradient structures. Post-processing via hot isostatic pressing and heat treatment achieves high specific strength, low elastic modulus, and good ductility. Furthermore, the gradient lattice effectively simulates the natural bone in terms of anisotropy, compressive strength, and biocompatibility.

2.5 Bionic lattice

During the extensive process of biological evolution, organisms have developed unique structures to adapt to their environments[44–45]. These structures and functions have undergone environmental selection and verification, providing a direct and effective template for the design of biomedical scaffold structures and generating many bionic structures[46–47].

Based on the crystal microstructure of metals and bamboo[26], porosities of 78.4% and 75.8% are preferred for bone implants, which demonstrates their potential to mimic the mechanical characteristics of cortical bone[48]. Qi et al[49] designed a structure that incorporates composite biomimetic features inspired by beetle elytra and cuticles. This structure offers significant mechanical advantages over traditional fcc and bcc structures as the implant.

Overall, the structural characteristics of bone implants have a significant impact on the performance of the structure. The more similar the design of an implant aligns with the natural structural characteristics of human bone, the closer its performance approximates that of human bone. Most research teams opt for forward design, using a specific basic structure or biomimetic sources to replicate the relevant properties of human bone, thereby achieving considerable mechanical properties[31,42]. Conversely, the reverse design method offers greater specificity than the forward design, allowing the structural features to more accurately reflect natural bone characteristics from the outset. This approach provides substantial advantages in the tailored structural design of medical implants.

It is worth noting that nowadays, the structural research of most teams in the field of biomedical bone implants focuses on proposing design methods that are similar to natural bone structures, and has established quantitative relationships between the geometric parameters and mechanical properties of the structures, including superelasticity and shape-memory performance. Some structures have formed systematic design methods. As for another important performance of bone implants, namely biocompatibility, some teams have effectively restricted the release of Ni^+ by surface treatment technique and effectively improved the biocompatibility of NiTi shape-memory alloy[50] nowadays. However, from the structural perspective, there are relatively few studies on constructing the quantitative relationship combination of structural parameters and biocompatibility to achieve a more parametric optimization process. Most studies still focus on the qualitative research of its relationship with structural parameters, using a restricted number of groups to reveal the variation law of biocompatibility with structural porosity and pore size within a restricted range. Zheng et al[51] investigated the effects of different pore diameters and porosity on the compatibility of NiTi porous structure with osteoblasts, sought

the optimal pore structure for orthopedic implants, and revealed that a pore diameter of 277 – 340 μm is the most suitable, and the smaller the pore diameter, the better the cell adhesion and proliferation effects. Lu et al[52] kept the porosity of 66% unchanged and studied the effect of pore size on the biocompatibility of the structure. The results showed that the pore size of 618 μm has the best effect on cell adhesion and mutual ligation, which better promotes the therapeutic effect of the implant. However, the quantitative mathematical relationship between biocompatibility and structural porosity, pore size, or other structural parameters has rarely been discussed. Such results are restricted by the complexity of factors affecting the biocompatibility of bone implants, including the proportion of NiTi alloy components and structural manufacturing precision, making the performance unpredictable. How to establish a quantitative mathematical relationship between structural parameters, such as porosity and pore size, and the cell survival rate achieved by the structure remains a key point for future research.

3 Engineering Field: Structures of Energy-Absorbing Component

The superelasticity and hysteresis of NiTi alloy arise from complex phase transition processes. As illustrated in Fig. 5, when the temperature exceeds the transition starting temperature of austenite phase (A_f), NiTi alloy is initially transformed from austenite to detwinned martensite during a load-and-unload cycle[53].

During this process, NiTi alloy exhibits a minimal irreversible strain while demonstrating remarkable spring-like elasticity. This characteristic endows NiTi structures with excellent reusability after deformation under external loads. Furthermore, the substantial hysteresis loop produced during the phase change process contributes to outstanding energy dissipation and significant damping performance of NiTi alloy, which has attracted extensive attention in the structural design of energy-absorbing components in engineering fields[3].

This section reviews the new structural design approaches for energy-absorbing components, discusses the performance advantages of the lattice and honeycomb structures, and demonstrates the application potential compared to that of existing structures. Table 4 and Table 5 show the structural features and important performances of each structure.

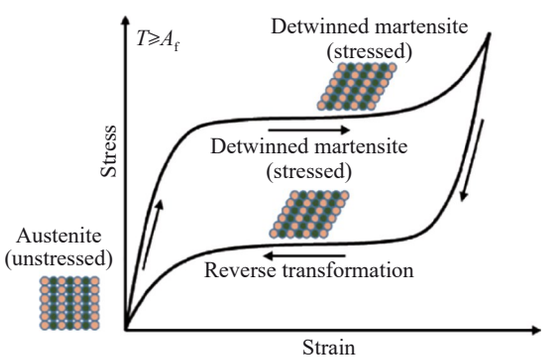

Fig.5 Schematic diagram of superelasticity and hysteresis characteristics of NiTi alloy[53]

3.1 Lattice structure

3.1.1 Truss lattice

Truss lattice structures are widely applied in engineering structural design due to their simple design principles and high degree of design freedom. A truss lattice structure with a high negative Poisson's ratio of −2.089 has been developed for military bulletproof equipment[54]. The finite element model confirms that the energy absorption of this structure is approximately twice that of a solid NiTi plate and about five times that of a solid steel plate. This advancement significantly enhances the dissipation efficiency of high-speed impact loads and provides a new approach to the lightweight design of bulletproof equipment. Biasutti et al[55] designed a NiTi truss lattice made up of octahedral cells for dampers, achieving optimal damping performance by tripling the height of the structure. The electroplated structure demonstrates excellent superelasticity. This stable energy dissipation mechanism provides a reliable solution for vibration attenuation under high-direction shock loads.

3.1.2 Hybrid lattice

The approach of integrating multiple high-performance elementary structures is also applicable to engineering fields, combining the high energy absorption, load-bearing capacity, and deformation recovery performance of various structures to achieve more optimal comprehensive properties.

Inspired by the frustule of the campylodiscus diatom[56], four structures were designed with varying ratios of traditional sharp angle (TSA) to bionic arc angle (BAA). And the structure with a TSA-to-BAA ratio of 0∶6 exhibits the highest deformation recovery rate (>99%).

Notably, the deformation and energy absorption performance of the structure can be significantly enhanced through macrostructural design methods that inhibit the formation of microscopic local deformation zones[57]. The helical lattice structure (HLS) of NiTi alloy is developed to effectively mitigate the adverse effects of local deformation bands on the deformation recovery performance of the structure, demonstrating stronger damage tolerance and more durable energy absorption characteristics under high compressive strain (40%–70%).

3.1.3 Gradient lattice

In the design of energy-absorbing components within the engineering field, gradient design approach enables the alteration of structural parameters both internally and externally, including wall thickness, pore diameter, and structural type. In this way, different areas can effectively leverage their respective advantages during energy absorbing process in impacts, thereby maximizing the overall performance of the structure[63–64].

Fig. 6 shows the topology optimization method to design four gradient lattice structures (GLS)[65]. The structures include unidirectional GLS, bi-directional increasing GLS, bi-directional decreasing GLS, and none-GLS. And the GLS

Table 4 Structure features and key performances of lattice structures of energy-absorbing components

Structure feature	Key performance	Ref.
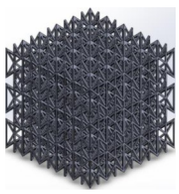	The specific energy absorption of the structure is 495 J·g^{-1}, which is 5.42 times and 1.96 times that of solid steel plate and solid NiTi plate, respectively. The structure can withstand the impact of a bullet of 875 m/s.	[54]
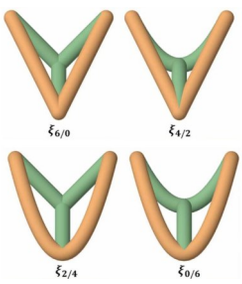	The $\xi_{0/6}$ structure exhibits the highest deformation recovery rate (>99%) and the lowest cumulative residual strain (0.83%) after 5 compression cycles, with an elastic modulus of 1.19 GPa.	[56]
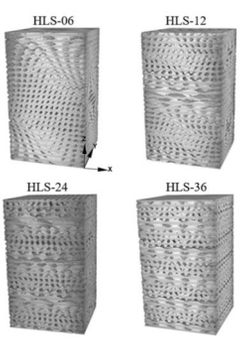	The specific energy absorption of the structure can reach up to 55 kJ·kg^{-1}. The structure can reach 100% deformation recovery after 10 compression cycles. The HLS-36 structure has a stable recoverable strain of up to 4.32%. The influence formula between the interlayer rotation angle θ and the structural performance is established.	[58]
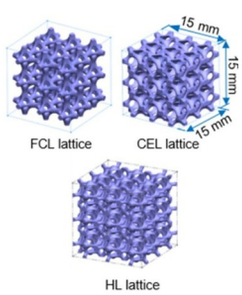	The specific compressive strength of HL structure is 41.74 MPa·cm^3·g^{-1}, and the specific energy absorption is 6.82 J/g. HL structure exhibits the best energy absorption capacity, with a hysteresis area of 0.12 J/g and a specific damping capacity of 0.14. HL structure has the highest deformation recovery rate of 85%.	[30]
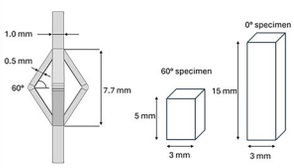	The best damping performance is obtained after the height and size of the structure are increased by 3 times. The superelastic deformation recovery rate is 90%.	[55]
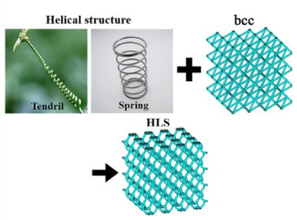	Under the compressive strain of 40%, the local strain of HLS (ε_{local}) is 7.5%. After 2 compression cycles at strain of 70%, HLS exhibits more stable specific energy absorption and ultimate stress than bcc structure.	[57]
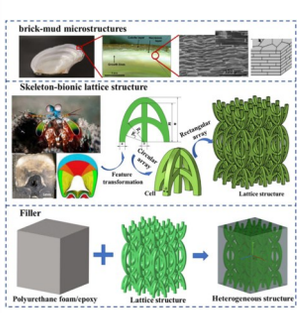	HS-EP composed of epoxy resin metal lattice structure has the highest specific strength of 57.34 MPa·cm^3·g^{-1} and specific energy absorption of 30.75 J/g. Applied to the field of sound absorption, the sound absorption coefficient reaches the highest of 0.78 when the sound wave frequency is 6000 Hz.	[8]

Note: the symbols and abbreviations in Table 4 are explained in the corresponding references.

structure with bi-directional increasing porosity gradient exhibits the highest energy absorption capacity.

In addition, a further exploration was conducted based on the topology optimization design method[30]. A force of 5000 N was applied at a 45° angle at the corner of the structural cube, after which the structural cube underwent three distinct loading conditions, including fixed center loading (FCL), center edge loading (CEL), and hybrid loading (HL), as illustrated in Fig. 7[30]. It has been confirmed that HL structure exhibits the best overall performance due to its layer-by-layer deformation mechanism.

This approach presents a viable design method for application fields that have specific requirements regarding structural stress conditions.

3.1.4 Hierarchical lattice

Hierarchical lattices are structures in which the constituent units are arranged in layers along a specific direction. The overall structure is governed by parameters, such as the angle between the layers and the ordering of these layers[35], which is one of the parametric structures.

Ma et al[58] developed a spiral hierarchical lattice characterized by exceptional superelasticity and energy absorption capacity, inspired by the biological structure of spiral hierarchies. Furthermore, a formula is established to

Table 5 Structure features and key performances of honeycomb structures of energy-absorbing components

Structure feature	Key performance	Ref.	Structure feature	Key performance	Ref.
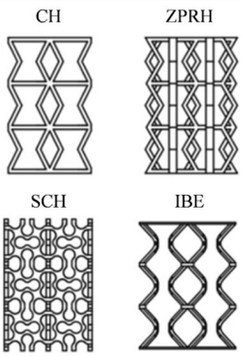	IBE structures have the best deformation recovery rate of 99.7%, and the deformation recovery rate of all structures is between 98.5%–99.7%.	[59]	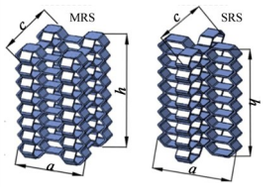	MRS structure (MRS-T4A6) with a thickness of 0.45 mm and an angle of 60° has the highest specific energy absorption of 10.4 J/g. The mean crushing force is 3.05 kN at the highest level.	[60]
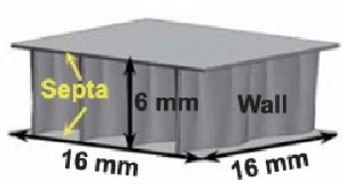	The bionic hybrid structure (BHS) can bear more than 25 000 times the weight of itself. BHS has a specific energy absorption of 5.32 J/g, and the deformation recovery rate after heating is 99.1%.	[9]	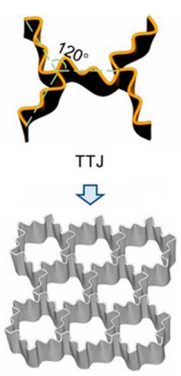	When the ratio of the wall thickness of the upper and lower surfaces (α) of the double triple-junction (TTJ) structure is 2/3, it has the maximum specific compressive strength of 70.64 MPa·cm^3·g^{-1} and the specific energy absorption of 35.84 J/g. The structure with α of 1/3 has the highest specific energy absorption of 53.84 J/g.	[62]
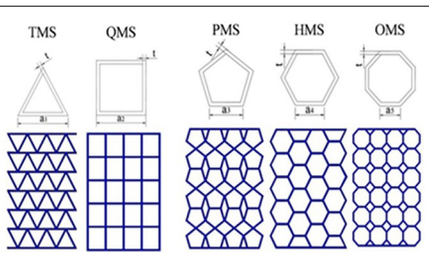	The specific energy absorption and mean crushing force of the pentagonal cell structure are 3.331 J/g and 3165.74 J/kg, respectively. The deformation recovery rate after heating is up to 98%.	[61]			

Note: the symbols and abbreviations in Table 5 are explained in the corresponding references.

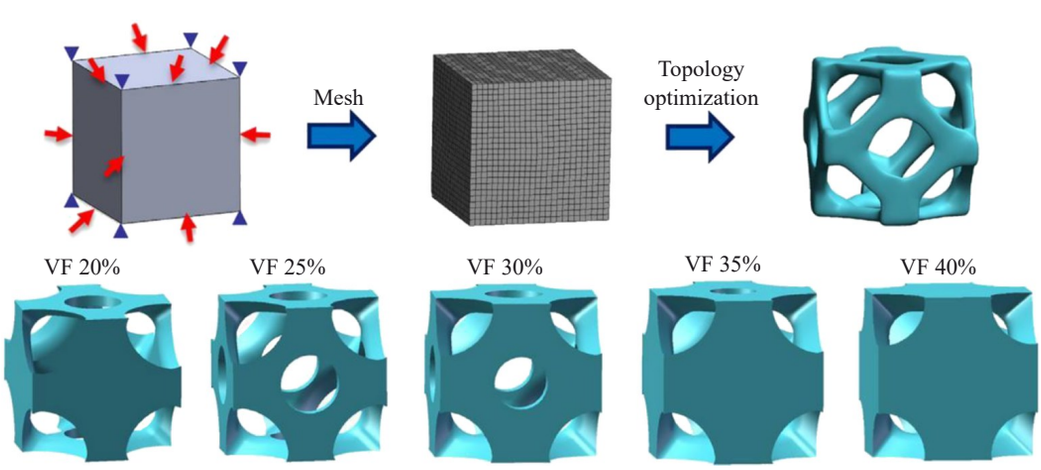

Fig.6 Modeling process using topology optimization[65] (VF means volume fraction)

quantify the influence of interlayer rotation angle (θ) on molding accuracy, deformation behavior, and fracture form, thereby elucidating the quantitative relationships between structural parameters and their properties. This work provides a parametric design paradigm for structures in the domain of high-performance energy absorption.

3.1.5 Heterogeneous lattice

Heterogeneous lattices are structures composed of unevenly

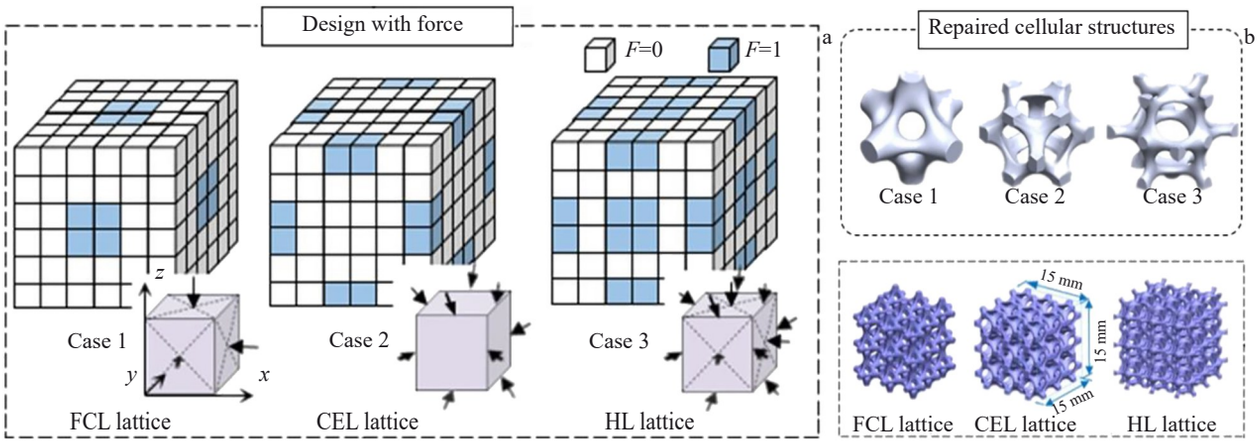

Fig.7 Topology optimization design methods and resulting models driven by different loading conditions[30]: (a) schematic diagrams of FCL, CEL, and HL lattices (F=0 indicates no applied force, and F=1 indicates applied force); (b) topology optimization methods and corresponding resulting models

distributed cell elements, materials, and processing techniques. This type of structure expands the basic elements involved in hybridization from different structures to different materials and process levels compared with hybrid lattice, offering higher design freedom[35].

Yu et al[8] were inspired by the characteristics of the skeleton-filling from a nacre shell and the cross-sectional morphology of the dactyl club from mantis shrimp, using organic polymers (polyurethane PU or epoxy resin EP) and scaffold structures to create heterogeneous lattices applicable in sound absorption and noise reduction engineering.

3.2 Honeycomb structure

The integration of NiTi alloy with honeycomb structures by various research teams has resulted in enhanced shape-memory effects and superelasticity, demonstrating superior shape recovery capabilities compared to honeycomb structures made from other materials[66–67]. This allows the application field of the honeycomb structure to be broadened again. On the basis of the original high energy absorption capacity, it is further optimized and has excellent repurposing.

Inspired by traditional honeycomb structures and beetle elytra structures, four bionic structures were designed[59]. This study provides valuable insights for the design of recoverable energy-absorbing structures in satellite landing scenarios. Yu et al[60] designed two types of bionic honeycomb structures, multi-rotation structure (MRS) and single rotation structure (SRS), which are suitable for developing efficient and self-recovering new protective structures in the fields of vehicle armor and aerospace. Liu et al[61] designed a series of honeycomb structures composed of polygonal cells. Experiments and finite element simulations verify that the pentagonal cell honeycomb structure has the best overall performance[68].

Fig. 8 shows the bionic principle of the high-performance honeycomb structure designed by Yuan et al[62] based on cuttlebone. Initially, they proposed a novel BHS that reflects the overall patterns of the bone cross-section. The irregular distribution curve observed in the cross-section of the squid bone was modeled using the sum of double sinusoidal functions. Experimental validation demonstrated that BHS exhibits excellent bearing capacity, energy absorption capacity, and good reusability[9]. Subsequently, based on this research, a TTJ structure with gradient wall thickness was designed to accommodate the local patterns of the bone cross-section. It was confirmed that when the gradient parameter (α), as defined in Fig.8d, is set to 2/3, the structure can exhibit the best energy absorption capacity. This investigation reveals that the gradient design facilitates a layer-by-layer failure mechanism within the structure[62]. Consequently, a high-performance bionic honeycomb structure has been developed based on these two aspects.

Compared to lattice structures, honeycomb structures exhibit superior energy absorption and bearing capacity[69–70]. This advantage is partly attributed to their effective stress dispersion capabilities and isotropic properties, which ensure consistent mechanical performance in all directions while minimizing local variations[71–72]. Typically, the design of honeycomb structures involves adjusting wall thickness and cell size, which is a conventional method that may result in increased mass compared to lattice structures optimized through topological methods[73]. Future research should focus on reducing cell size to enhance the strength-to-mass ratio.

4 Future Prospects

The development of additive manufacturing technique has promoted the development of NiTi alloy with high-performance porous structures towards greater complexity and functionality. In future structural design, it is more important to establish a highly credible mapping relationship between structural features and performance, so as to achieve high-precision parameterization of structural design.

On the one hand, the performance of the structure can be predicted through the designed structural parameters during the forward design process, thereby reducing the need for unnecessary experimental verification and associated costs. On the other hand, it allows for the reverse matching of appropriate structural parameters based on specific

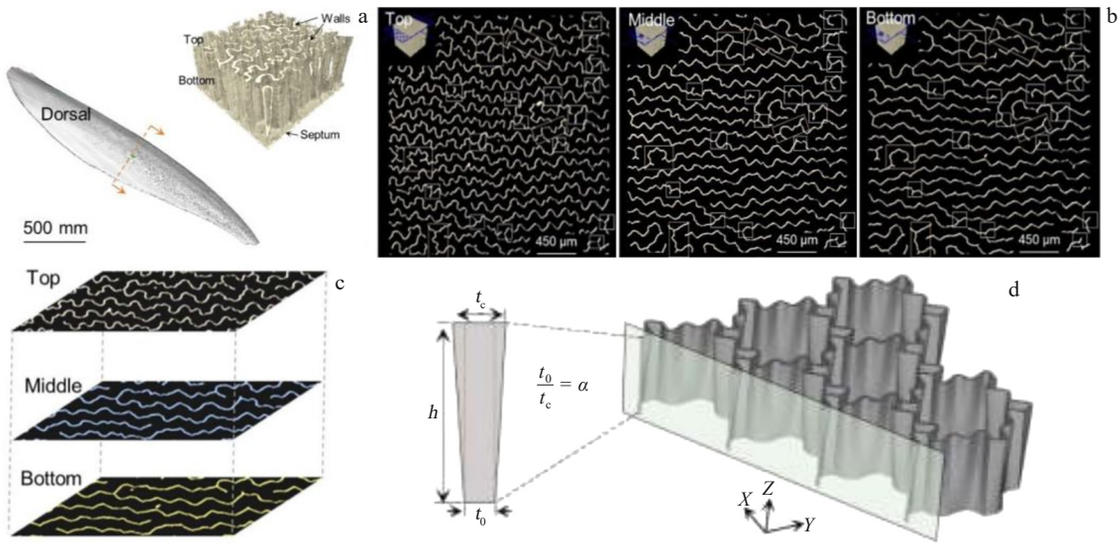

Fig.8 Principles and methods of biomimetic design of honeycomb structure based on cuttlebone[62]: (a) biological structure of cuttlebone; (b) stripe features of cuttlebone section; (c) characteristics of top, middle, and bottom cross-section of cuttlebone; (d) definition of gradient parameters

requirements, which is particularly advantageous in the structural design of medical implants. However, the practical application of parametric structure design relies heavily on extensive experimentation, and the analysis of complex relationships among large datasets often leads to a significant barrier to the process of structural parameterization.

Notably, machine learning (ML) can process complex data and reveal potential relationships or rules between data that conventional methods cannot analyze. ML can learn from historical data, identify and judge various complex information that may be overlooked, and provide the necessary foundational data according to the generated dataset[69]. The integration of ML with the parametric structural design process offers significant advantages in addressing the complex mapping between structural parameters and performance[70]. The relevant process is illustrated in Fig.9[74]. Based on the constructed dataset of structural parameters and performance, a training model was developed to predict the compressive performance and superelasticity of structures designed according to the lattice characteristics of austenite and martensite. The high-performance structure exhibits a compressive strength ranging from 20.39 MPa to 220.92 MPa, with a superelastic deformation recovery rate of 99.35%.

Furthermore, for the deficiencies in the quantitative research on the structural biocompatibility of the aforementioned bone implants, ML can play an effective promoting role. Under the same cell experimental conditions, by altering various possible influencing factors and setting up experimental groups, the cell survival rate can be used as the label quantity, and various influencing factors are used as the feature quantity, revealing potential data relationships and training ML models. Then, through the result evaluation and model optimization of interpretable ML, it can provide new ideas for establishing the quantitative relationship between structural parameters, such as biocompatibility and porosity of bone implants.

Although ML has demonstrated significant value in the process of mapping the parameters and properties of porous structures in NiTi alloys, its practical application still faces multiple bottlenecks. Firstly, the quantity of foundational data in this process and the learning outcomes exhibit a strong dependency, necessitating large-scale and high-quality datasets. This poses a high cost for the additive manufacturing process and mechanical property testing required for porous structures in NiTi alloys, and fluctuations in the manufacturing process can also lead to data deviations. Additionally, the impact of extreme working conditions on structural performance is often an uncontrollable variable, restricting the generalization ability of model[75]. Secondly, the majority of ML models suffer from the black box effect, meaning that it is difficult to clearly elucidate how the learning and prediction outcomes are derived from the original data, which restricts the reliability of the models[76]. Furthermore, ML models exhibit insufficient learning capabilities with small sample sizes. And in application scenarios with customized requirements, such as NiTi alloy bone implants, ML models are prone to overfitting, leading to reduced prediction accuracy[77]. It is noteworthy that cross-scale molecular dynamics (MD) simulations can facilitate the ML process. Cross-scale MD simulations can reveal the phase transformation mechanisms of NiTi alloys from the atomic scale and correlate the microscopic atomic behavior with the macroscopic structural properties of NiTi alloys, such as superelasticity and shape-memory effects, through methods like coarse-grained models. This provides high-fidelity virtual datasets for ML models, compensating for the lack of experimental data[78]. Specifically, at the atomic scale, the ReaxFF force field can be used to simulate the chemical

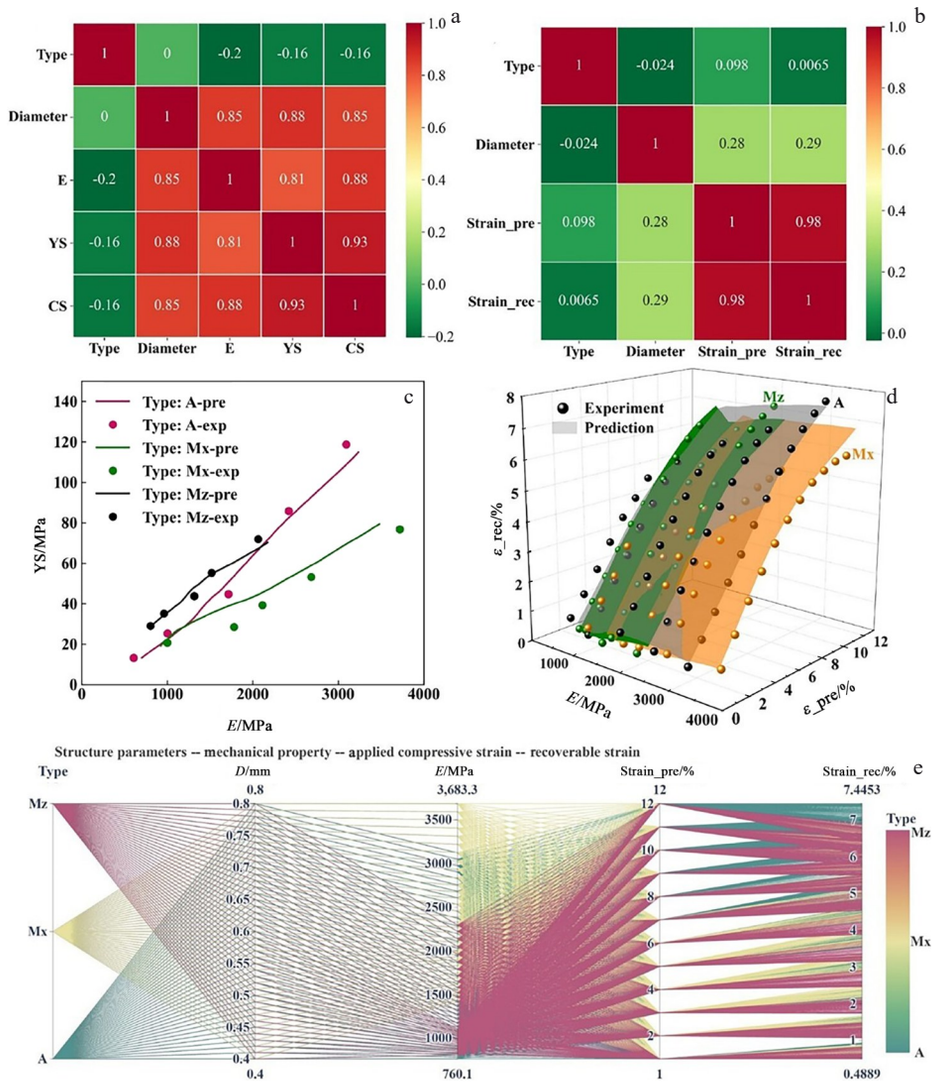

Fig.9 Construction and application process of ML model[74]: (a) Pearson correlation coefficient among structural type, diameter, and mechanical properties (E, YS, CS); (b) Pearson correlation coefficient among structural type, diameter, applied compressive strain, and recoverable strain; (c) comparison of mechanical properties (YS and *E*) between predictions and experiments; (d) comparison of recoverable strain of NiTi microlattice between the experiments and predictions; (e) parallel coordinate plot for predicted mechanical properties and recoverable strain with different combinations of structural types and diameters of NiTi microlattice (the symbols and abbreviations in Fig. 9 are explained in the Ref.[74])

bonding interactions and phase transition dynamics between NiTi alloy atoms, thereby obtaining fundamental parameters, such as elastic modulus and phase transition temperature under different lattice structures. At the mesoscale, the discrete element method can be employed to treat atomic clusters as basic units, simulating the evolution of porosity in porous structures. Finally, at the macroscopic scale, finite element analysis can be integrated to output the overall mechanical response of the structure[79]. The multi-dimensional data generated from these cross-scale simulations, including stress-strain curves and structural porosity, can be used to expand the ML training dataset. This significantly enhances the ability of models to learn the relationship between structure and performance in parameter ranges that are difficult to cover experimentally[80], and it also reduces the learning costs. Additionally, cross-scale MD simulations can compare the mechanical behavior of NiTi alloys under specific structural parameters with ML predicted values, thereby enabling the reverse optimization of model parameters and providing a reliable pathway for the high-precision parametric design of porous structures in NiTi alloys.

5 Conclusions

1) The research progress of porous NiTi shape-memory alloy structures fabricated by SLM in the biomedical and engineering fields was reviewed. In the biomedical field, innovative structures, including truss lattice, fractal lattice, hybrid lattice, gradient lattice, and bionic lattice, have effectively addressed issues, such as elastic modulus mismatch with natural human bone and insufficient

biocompatibility of traditional bone implants, enabling excellent osteocyte activity and achieving better therapeutic outcomes.

2) In the mechanical engineering field, the superelasticity and shape-memory effect of NiTi alloy enable lattice and honeycomb structures to demonstrate outstanding energy absorption capacity, deformation recovery performance, and reusability. The incorporation of NiTi alloy and various innovative design methods for porous structures provide novel design strategies for bulletproof equipment, dampers, and aerospace protective structures.

3) It is noteworthy that with the support of technique, such as ML and cross-scale MD simulations, the complex mapping relationships between structural parameters and performance are expected to be established, promoting the development of NiTi porous structures toward greater customization and further expanding their application prospects in high-end medical implants and advanced engineering structures.

References

1 Sabahi N, Chen W L, Wang C H *et al. JOM*[J], 2020, 72(3): 1229

2 Alagha A N, Hussain S, Zaki W. *Materials & Design*[J], 2021, 204: 109654

3 Dzogbewu T C, de Beer D J. *Heliyon*[J], 2024, 10(1): e23369

4 Elahinia M H, Hashemi M, Tabesh M *et al. Progress in Materials Science*[J], 2012, 57(5): 911

5 Zhao M, Qing H B, Wang Y X *et al. Materials & Design*[J], 2021, 200: 109448

6 Attaran M. *Business Horizons*[J], 2017, 60(5): 677

7 Zhang Y T, Wei D X, Chen Y *et al. Journal of Materials Science & Technology*[J], 2024, 186: 48

8 Yu Z L, Chen L X, Zhang C L *et al. Composites Science and Technology*[J], 2024, 256: 110765

9 Yuan L H, Gu D D, Liu X *et al. International Journal of Extreme Manufacturing*[J], 2024, 6(5): 055001

10 Wen S F, Gan J, Li F *et al. Materials*[J], 2021, 14(16): 4496

11 Amadi A, Mohyaldinn M, Ridha S *et al. Journal of Alloys and Compounds*[J], 2024, 976: 173227

12 Xue L, Atli K C, Zhang C *et al. Acta Materialia*[J], 2022, 229: 117781

13 Parvizi S, Hashemi S M, Asgarinia F *et al. Progress in Materials Science*[J], 2021, 117: 100739

14 Chen L, Deng C J, Li J Y *et al. Biomaterials*[J], 2019, 196: 138

15 Feng J Y, Wei D X, Zhang P L *et al. Journal of Manufacturing Processes*[J], 2023, 85: 160

16 Zhang T, Wei D X, Lu E Y *et al. Journal of Materials Science & Technology*[J], 2022, 131: 68

17 Poudel I, Annaji M, Zhang C *et al. Molecular Pharmaceutics*[J], 2023, 20(8): 4236

18 Xu S B, Zhang S, Ren G C *et al. Materials*[J], 2022, 15(17): 5896

19 Mishra R K, Singh S S. *Multiscale and Multidisciplinary Modeling, Experiments and Design*[J], 2024, 8(1): 67

20 Aufa A N, Hassan M Z, Ismail Z *et al. Progress in Additive Manufacturing*[J], 2024, 10(4): 2247

21 Wang X J, Xu S Q, Zhou S W *et al. Biomaterials*[J], 2016, 83: 127

22 Kujala S, Ryhänen J, Danilov A *et al. Biomaterials*[J], 2003, 24(25): 4691

23 Hariharan A, Goldberg P, Schell F *et al. Advanced Functional Materials*[J], 2023, 34(8): 2310607

24 Hauschwitz P, Klicova M, Mullerova S *et al. Biomedical Materials*[J], 2023, 18(4): 045008

25 Levin M, Spiro R, Jain H *et al. Medical Devices: Evidence and Research*[J], 2022, 5: 103

26 Zhang X L, Jiang Y, Wang S P *et al. Acta Metallurgica Sinica* (*English Letters*)[J], 2023, 36(6): 926

27 Ungár T, Frenzel J, Gollerthan S *et al. Journal of Materials Research*[J], 2017, 32(23): 4433

28 Kubášová K, Drátovská V, Losertová M *et al. Materials*[J], 2024, 17(6): 1248

29 Jin J L, Wu S Q, Yang L *et al. International Journal of Machine Tools and Manufacture*[J], 2024, 195: 104099

30 Liu X, Gu D D, Yuan L H *et al. Virtual and Physical Prototyping*[J], 2024, 19(1): e2365860

31 Kong D, Wang Q, Huang J *et al. Advanced Functional Materials*[J], 2023, 34(8): 2305412

32 Kang J F, Dong E C, Li D C *et al. Materials & Design*[J], 2020, 191: 108608

33 Farber E, Orlov A, Borisov E *et al. Metals*[J], 2022, 12(9): 1476

34 Zhang X D, Yang F, Liu B S *et al. Modelling and Simulation in Materials Science and Engineering*[J], 2021, 29(8): 084001

35 Ma W W S, Yang H, Zhao Y *et al. Advanced Science*[J], 2025, 12(8): 2405835

36 Fu J, Qu S, Ding J H *et al. Additive Manufacturing*[J], 2021, 44: 102067

37 Wang Y J, Wen W L, Wu S *et al. Remote Sensing*[J], 2018, 11(1): 63

38 Kolken H M A, Janbaz S, Leeflang S M A *et al. Materials Horizons*[J], 2018, 5(1): 28

39 Zadpoor A A. *Acta Biomaterialia*[J], 2019, 85: 41

40 Huang Y, Zhai L L. *Scientific Reports*[J], 2025, 15(1): 11026

41 Li F L, Gan J K, Zhang L *et al. Composites Science and Technology*[J], 2024, 245: 110365

42 Kong D Y, Wang Q, Huang J G *et al. Computers in Biology and Medicine*[J], 2023, 165: 107369

43 Tan C L, Zou J, Li S *et al. International Journal of Machine Tools and Manufacture*[J], 2021, 167: 103764

44 Lee S S, Du X, Kim I *et al. Matter*[J], 2022, 5(9): 2722

45 Yang W B, Han Q, Chen H *et al. Journal of Materials Science & Technology*[J], 2024, 188: 116

46 Huang T S, Mao Z Y, Chang L J *et al. Journal of Bionic Engineering*[J], 2023, 20(5): 1942

47 Liang H Y, Zhao Y, Chen S X *et al. Automotive Innovation*[J], 2023, 6(3): 379

48 Nikolov S, Petrov M, Lymperakis L *et al. Advanced Materials*[J], 2010, 22(4): 519

49 Qi Y C, Chi H J, Liu X *et al. Thin-Walled Structures*[J], 2025, 208: 112817

50 Zhang Gang, Tian Zhuoyuan, Shi Yu *et al*. *Rare Metal Materials and Engineering*[J], 2025, 54(5): 1353 (in Chinese)

51 Zheng J, Jian Y T, Yang Y *et al. Plos One*[J], 2015, 10(6): e0128138

52 Lu H Z, Ma H W, Luo X *et al. Journal of Materials Research and Technology*[J], 2021, 15: 6797

53 Seo J, Kim Y, Hu J. *Applied Sciences*[J], 2015, 5(3): 187

54 Hassanin H, Abena A, Elsayed M A *et al. Micromachines*[J], 2020, 11(8): 745

55 Biasutti T, Bettini P, Grande A M *et al. Progress in Additive Manufacturing*[J], 2025, 10: 6151

56 Sun J, Gu D, Lin K *et al. Smart Materials and Structures*[J], 2022, 31(7): 074003

57 Zhou M, Li H H, Xiong Z W *et al. Journal of Materials Science & Technology*[J], 2025, 217: 237

58 Ma C L, Peng X, Zhu D H *et al. Journal of Manufacturing Processes*[J], 2023, 108: 610

59 Yu Z L, Xin R L, Xu Z Z *et al. Journal of Bionic Engineering*[J], 2022, 19(6): 1684

60 Yu Z L, Chen L X, Xin R L *et al. Materials Today Communications*[J], 2022, 33: 104313

61 Liu Z X, Liu W D, Ma W J. *AIP Advances*[J], 2022, 12(7): 075201

62 Yuan L H, Gu D D, Lin K J *et al. Virtual and Physical Prototyping*[J], 2024, 19(1): e2321160

63 Chen W, Chen C, Zhang Y H *et al. Engineering Fracture Mechanics*[J], 2025, 320: 111077

64 Zhang P, Qi D X, Xue R *et al. Composite Structures*[J], 2021, 277: 114606

65 Chen W, Gu D D, Yang J K *et al. International Journal of Extreme Manufacturing*[J], 2022, 4(4): 045002

66 Tamburrino F, Graziosi S, Bordegoni M. *Journal of Computing and Information Science in Engineering*[J], 2018, 18(4): 040801

67 Isaac C W, Duddeck F. *Virtual and Physical Prototyping*[J], 2023, 18(1): e2197436

68 Balasubramaniam S, Selvam M, Manickam R *et al. Construction and Engineering Structures*[J], 2023, 2(1): 1

69 Li L B, Yang F, Zhang S Y *et al. Engineering Structures*[J], 2023, 289: 116335

70 Zhang L, Song B, Zhao A G *et al. Composite Structures*[J], 2019, 226: 111199

71 Li Z, Kang Z, Su X. *Machines*[J], 2023, 11(2): 294

72 Singh O, Behera B K. *Journal of Composite Materials*[J], 2024, 58(14): 1619

73 Hao J, Wu X, Oporto G *et al. European Journal of Wood and Wood Products*[J], 2020, 78(6): 1195

74 Zhang Z, Gao J B, Wei S S *et al. Virtual And Physical Prototyping*[J], 2025, 20(1): e2444572

75 Mehrpouya M, Gisario A, Nematollahi M *et al. Materials Today Communications*[J], 2021, 26: 102022

76 Sawada Y, Nakamura K. *IEEE Access*[J], 2022, 10: 41758

77 Parvizi S, Hafizpour H R, Sadrnezhaad S K *et al. Powder Metallurgy*[J], 2013, 54(3): 450

78 Tang H, Zhang Y, Li Q J *et al. Acta Materialia*[J], 2022, 238: 118217

79 Karamooz-Ravari M R, Shahriari B. *Meccanica*[J], 2018, 53(13): 3383

80 Khalvandi A, Saber-Samandari S, Aghdam M M. *Heliyon*[J], 2024, 10(7): e28995

NiTi形状记忆合金选区激光熔化多孔结构的设计、性能与多领域应用进展

马晓璐[1,2]，王偲宇[1]，沈渤然[1]，吴文征[1]，李桂伟[1]

(1. 吉林大学 机械与航空航天工程学院，吉林 长春 130025)

(2. 长春大学 机械与车辆工程学院，吉林 长春 130022)

摘　要：NiTi形状记忆合金凭借其独特的形状记忆效应与超弹性，已在多个领域得到广泛应用。增材制造技术实现了NiTi形状记忆合金高性能复杂结构精准成形，助力新型结构设计。本文回顾了选区激光熔化（SLM）制备的NiTi多孔结构在生物医学和机械工程领域的应用情况，综述了不同应用场景下各类新型SLM-NiTi多孔结构的特点，探讨了该类结构的创新性设计方法，并分析了其相应的优异性能，包括压缩性能、超弹性、形状记忆效应、能量吸收能力及生物相容性，为增材制造高性能NiTi结构的设计及应用提供参考。

关键词：NiTi形状记忆合金；选区激光熔化；多孔结构

作者简介：马晓璐，女，1989年生，博士生，吉林大学机械与航空航天工程学院，吉林 长春 130025，E-mail：xlma20@mails.jlu.edu.cn